Electronic Supplementary Material (ESI) for Analyst.

Supplementary information for:

Dielectrophoretic isolation of cells using 3D microelectrodes featuring castellated blocks

Xiaoxing Xing, and Levent Yobas*

Department of Electronic and Computer Engineering, Hong Kong University of Science and Technology, Clear Water Bay, Kowloon, Hong Kong

*Corresponding Author: eelyobas@ust.hk

Single-shell model

The dielectric properties of viable cells are approximated here by a single-shell model. The model treats the cytoplasm as a homogenous spherical body enveloped by a thin isotropic shell signifying the cell membrane and immersed in extracellular medium. According to the model, the effective complex permittivity of cells $\tilde{\varepsilon}_{cell}$ can be described as:[1]

$$\tilde{\varepsilon}_{cell} = \frac{\tilde{c}_{mem} R \tilde{\varepsilon}_c}{\tilde{c}_{mem} R + \tilde{\varepsilon}_c} \quad \text{(S–1)}$$

where $\tilde{\varepsilon}_c$ is the complex permittivity of the cytoplasm and $\tilde{c}_{mem}$ is the membrane complex capacitance stated as:

$$\tilde{c}_{mem} = c_{mem} + g_{mem}/j\omega \quad \text{(S–2)}$$

where c_{mem} and g_{mem} are the capacitance and conductance of cell membrane per unit area and related to the membrane permittivity ε_{mem} and conductivity σ_{mem}, respectively. The membrane conductance of viable mammalian cells (g_{mem}~10 S m^{-2} or less)[2,3,4] is negligible and thus, $f_{CM}(\omega)$, based on the above, becomes:

$$f_{CM}(\omega) = -\frac{\omega^2(\tau_m\tilde{\tau}_c - \tau_c\tilde{\tau}_m) + j\omega(\tilde{\tau}_m - \tilde{\tau}_c - \tau_m) - 1}{\omega^2(2\tau_m\tilde{\tau}_c + \tau_c\tilde{\tau}_m) - j\omega(\tilde{\tau}_m + \tilde{\tau}_c + 2\tau_m) - 2} \quad \text{(S–3)}$$

where all the time constants pertaining to the cytoplasm, membrane and immersion medium are accordingly defined: $\tau_c = \varepsilon_c/\sigma_c$, $\tilde{\tau}_c = \tilde{c}_{mem}R/\sigma_c$, $\tau_m = \varepsilon_m/\sigma_m$, and $\tilde{\tau}_m = \tilde{c}_{mem}R/\sigma_m$. For nonviable cells, however, the cell membrane becomes leaky exhibiting a conductivity increase by a factor of ~10^4 and hence can no longer be ignored.[2] $f_{CM}(\omega)$ is then evaluated as:

$$f_{CM}(\omega) = \frac{\varepsilon_c - \varepsilon_m + (\sigma_c - \sigma_m)/j\omega}{\varepsilon_c + 2\varepsilon_m + (\sigma_c + 2\sigma_m)/j\omega} \quad \text{(S–4)}$$

The real part of CM factor $Re[f_{CM}(\omega)]$ determines the direction and strength of the DEP force. At low frequencies ($\lesssim$ 100 kHz), the field lines cannot penetrate the cell membrane capacitance. Thus, the intact mammalian cells appear less polarizable than the immersion buffer and thus respond according to nDEP ($Re[f_{CM}(\omega)] < 0$). At intermediate frequencies (~0.1–100 MHz), however, the field lines bridge the membrane capacitance. Viable cells become more polarizable than the immersion buffer at a lower conductivity than their cytoplasm, thus experiencing pDEP ($Re[f_{CM}(\omega)] > 0$). In theory, the forces exerted by pDEP could reach twice as high levels as those by nDEP ($-0.5 \lesssim Re[f_{CM}(\omega)] \lesssim +1$). Between the two opposite cases, cells show no response to the field gradient at a particular crossover frequency, $f_0 = \omega_0/2\pi$, ($Re[f_{CM}(\omega)]$~0), which can be expressed for viable cells as:

$$f_0 = \frac{1}{2\pi}\sqrt{\frac{(\sigma_m - \sigma_{cell})(\sigma_{cell} + 2\sigma_m)}{(\varepsilon_{cell} - \varepsilon_m)(\varepsilon_{cell} + 2\varepsilon_m)}} \quad \text{(S–5)}$$

where $\sigma_{cell} = g_{mem}R$ and $\varepsilon_{cell} = c_{mem}R$ for a first crossover frequency whereas $\sigma_{cell} = \sigma_c$ and $\varepsilon_{cell} = \varepsilon_c$ for a second crossover frequency since the cell size and membrane properties dominate at low frequencies while those of the cytoplasm take over at high frequencies.

MATLAB (The Mathworks Inc.) was utilized to evaluate and plot the real part of the Clausius-Mossotti (CM) factor $Re[f_{CM}(\omega)]$ for viable and nonviable cells. The cell radius (R) was estimated to be 6.5 μm based on the imaging of viable cells through optical microscopy. Nonviable cells were also assumed to be at the same size since they did not show noticeable shrinkage or swelling. For both viable and nonviable cells, the membrane capacitance (c_{mem}) was set at 0.01 F/m^2. Although this value might have been altered for nonviable cells, the change was not trivial to predict and should not lead to a drastic variation in the overall plot.[4,5] The membrane conductance (g_{mem}) was assigned for viable and nonviable cells as 10 and 10^5 S/m^2, respectively. For viable cells, the conductivity and permittivity of the cytoplasm were $\sigma_c = 0.5$ S/m and $\varepsilon_c = 60\varepsilon_0$. For nonviable cells, the permittivity was not changed while the conductivity was altered because of their leaky membrane. Here, the conductivity of nonviable cells was set to values that concurred with their experimentally observed DEP polarity: 50, 150, and 1000 μS/cm, for a buffer at 17, 100, and 1000 μS/cm, respectively.

Computational modelling of electrical and fluidic domains

The electric potential distribution ϕ across the 3D array was obtained by solving Laplace equation $\nabla(\tilde{\sigma}_i \nabla\phi) = 0$ for the stated boundary conditions ($\tilde{\sigma}_i = \sigma_i + j\omega\varepsilon_i$ is the complex conductivity where the subscript i denotes the domain at a specified coordinate). The conductivity (σ_i) was set

at either 17, 100, or 1000 μS/cm for aqueous buffer and 1.5 S/cm for the 3D doped silicon electrodes. The electrical permittivity (ε_i) for buffer and the electrodes was, respectively, $80\varepsilon_0$ and $11.7\varepsilon_0$ with the permittivity of free space $\varepsilon_0 = 8.854 \times 10^{-12}$ F/m. The local electric field vector and its spatial derivative were evaluated based on the relations $E = -\nabla\phi$ and $\nabla E = \nabla(-\nabla\phi)$. The time averaged DEP force acting on a cell in buffer was given by $\langle F_{DEP} \rangle = \pi\varepsilon_m R^3 Re[f_{CM}(\omega)]\nabla(E \cdot E^*)$ where $\varepsilon_m = 80\varepsilon_0$ is the buffer permittivity.

The flow velocity field and the shear rate profile within the 3D structure were obtained by solving Navier-Stokes equation for an incompressible laminar flow. The viscosity (η) and density (ρ) of water inside the flow chamber were taken as 10^{-3} Pa s and 10^3 kg/m^3, respectively. All the chamber walls were subjected to no-slip boundary conditions. The inlet boundary was set to a constant velocity, up to 116 μm/s, which corresponds to the highest flow rate in experiments (0.25mL/h), while the outlet boundary was set to no viscous stress. The fluidic drag on cells was given by the Stokes' drag, $F_{drag} = 6\pi\eta R\upsilon$, where υ is the cell velocity with respect to the fluid.

Fig. S1 illustrates free-body diagram for a cell under positive DEP railed by the planar wall along the electrode edge that extends from the convex corner to the pore (the main text, Fig. 5). The distance d that identifies the possible trapping point along this path (AA' axis) was estimated by equating the force vectors acting on the cell in either direction. These vectors were evaluated based on x and y components of the simulated F_{DEP} and F_{drag}:

$$F_{drag\_AA'} = F_{drag\_x}\cos(\alpha) + F_{drag\_y}\cos(\beta) \quad \text{(S–6)}$$

and

$$F_{DEP\_AA'} = F_{DEP\_y}\cos(\beta) - F_{DEP\_x}\cos(\alpha) \quad \text{(S–7)}$$

The force orthogonal to the electrode's planar wall was not considered since the friction between the cell and the wall was omitted for simplicity.

Fabrication of the array

Fig. S2 describes the fabrication process in major steps applied on Si-glass composite substrates. The process began with an anodic bonding step involving a glass wafer 500 μm thick and a Si wafer 200 μm thick and with both sides polished (800 V, 420 °C, and 600 mbar). The latter was chosen at a resistivity of 0.5–1 Ω-cm and (100) oriented. Subsequently, a SiO_2 hard mask was deposited and dry etched through a resist pattern to delineate the electrodes and the flow chamber. After stripping off the resist, the silicon wafer was partially structured to a depth of ~50 μm through cyclic deep reactive ion etch (DRIE). The etched structure was then passivated with a tetraethylorthosilicate (TEOS) thin film, which was subsequently cleared off from the trench floors through directional etch. With the sidewalls passivated, the silicon bulk exposed on the trench floors was etched in SF_6 plasma, forming 60 μm large pores through the digits beneath the necked regions between the electrode units. Upon clearing off the remaining TEOS from the sidewalls in wet etch, a 210-cycle DRIE step was performed to completely isolate the counter electrodes, exposing the glass bottom and forming the flow chamber. A thin PDMS cover plate punched with fluidic access ports and electrical vias was secured on the flow chamber upon activating both the surfaces in oxygen plasma.

Supplementary Figure

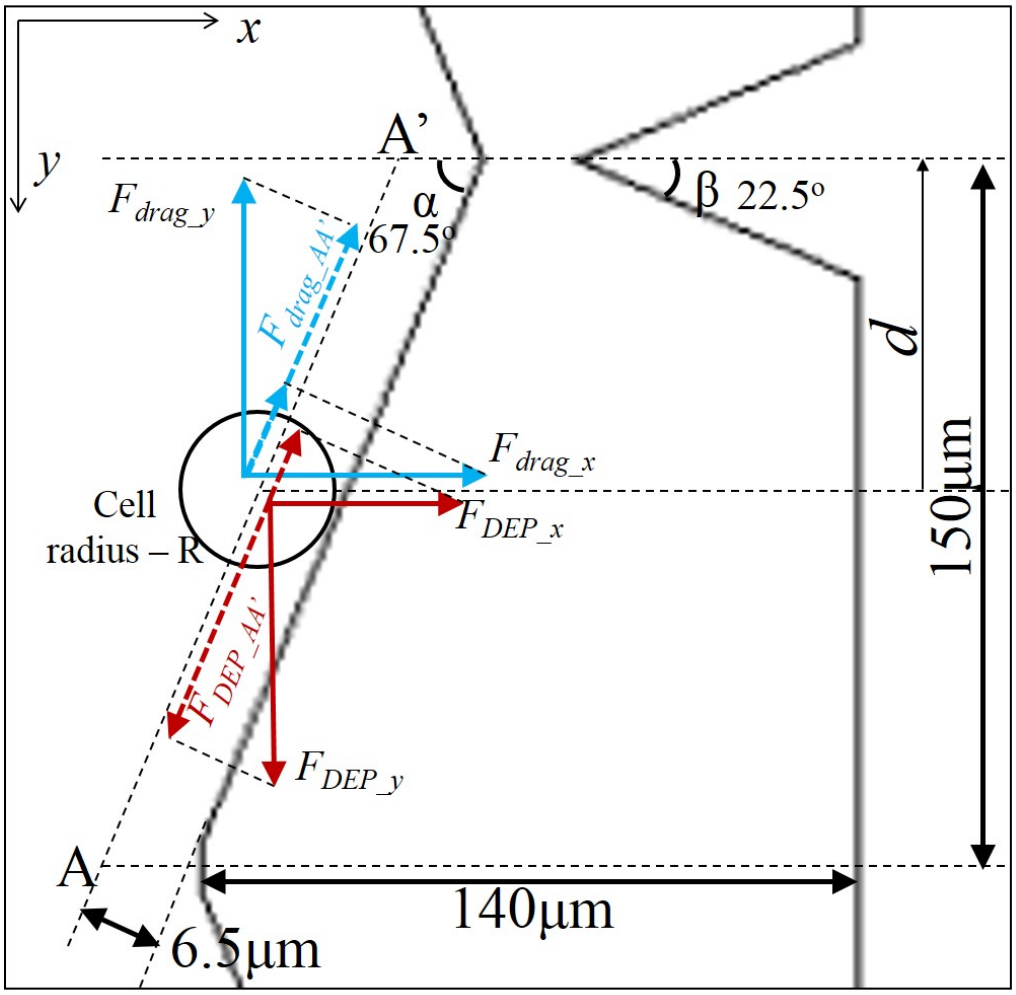

Figure S1: Free-body diagram illustrating the positive DEP and drag force vectors acting on the cell (F_{DEP} and F_{drag}). The trapping point lies at a projection distance d from the imaginary line that divides the electrode units.

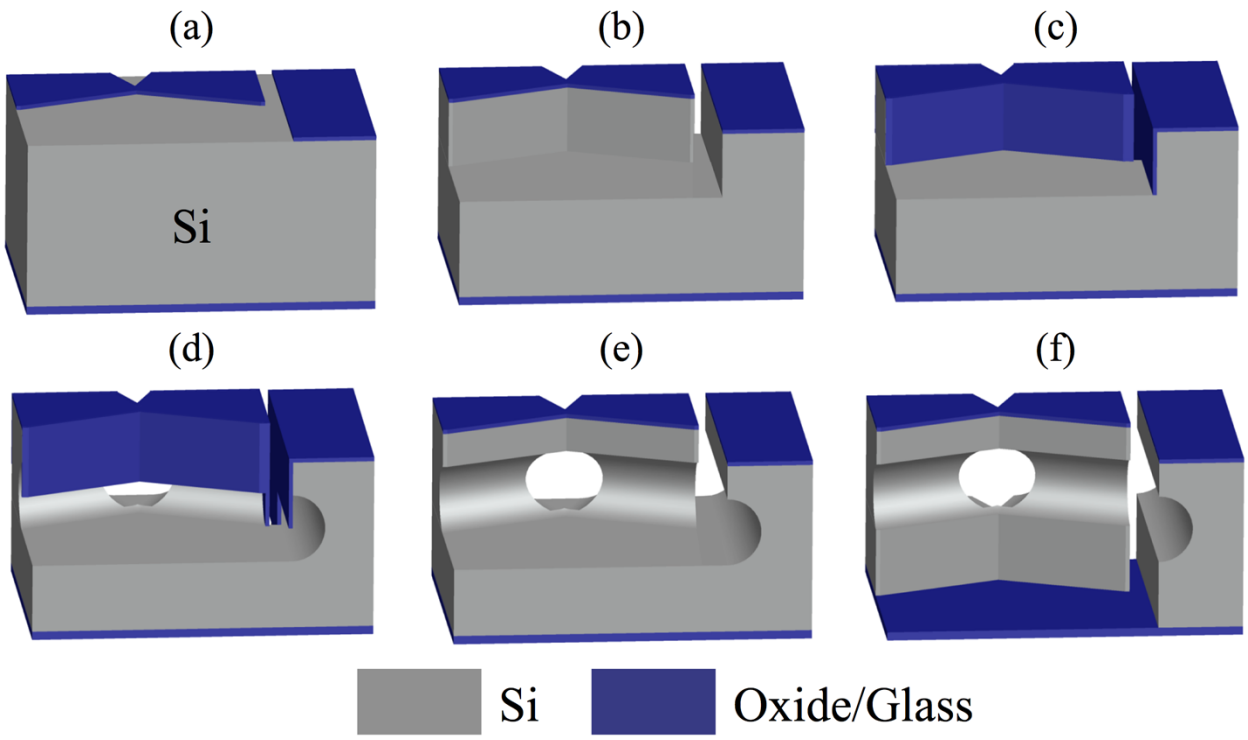

Figure S2: 3D renderings of major fabrication steps applied on Si-glass composite substrates: (a) depositing and patterning a SiO_2 hard mask to delineate the electrodes and the flow chamber; (b) Si DRIE cyclic etching; (c) depositing a thin film of tetraethylorthosilicate (TEOS) and then clearing it off from planar surfaces through directional etch; (d) Si isotropic etching through SF_6 plasma; (e) removing the sidewall TEOS in a wet etch; (f) Si DRIE cyclic etching down to the glass substrate and completely isolating the counter electrodes.

Supplementary Movie

Movie S1: Separation of live/dead cells.

The device section containing a 7-by-10 fluidic pore array (between the electrode units) undergoing a test with a binary mixture of viable (green) and nonviable (red) human colorectal carcinoma cells (HCT116) at a buffer conductivity of 1000 μS/cm and pressure injected from top to bottom at a rate of 0.2 mL/h. Viable cells can be seen captured (dashed circles) by the electrodes upon activation (±15 V_p 460 kHz) under relatively strong pDEP and then released upon deactivation. Nonviable cells are shown swept away owing to weak nDEP.

REFERENCES

1. T. B. Jones, *Electromechanics of Particles*, CAMBRIDGE University Press, 1995.
2. B. H. Lapizco-Encinas, B. A. Simmons, E. B. Cummings and Y. Fintschenko, *Anal. Chem.*, 2004, **76**, 1571-1579.
3. C. P. Jen and W. F. Chen, *Biomicrofluidics*, 2011, **5**, 044105.
4. F. Gielen, A. J. Demello and J. B. Edel, *Anal. Chem.*, 2012, **84**, 1849-1853.
5. R. Pethig and M. S. Talary, *IET Nanobiotechnol.*, 2007, **1**, 2-9.